Ultraviolet inverse photoemission and photoemission spectra of diluted magnetic semiconductor $Zn_{1-x}Mn_xTe$

1995 J. Phys.: Condens. Matter 7 4371

(http://iopscience.iop.org/0953-8984/7/23/008)

J. Phys.: Condens. Matter 7 (1995) 4371–4383. Printed in the UK

Ultraviolet inverse photoemission and photoemission spectra of diluted magnetic semiconductor $Zn_{1-x}Mn_xTe$

M Taniguchi†, N Happo†, K Mimura†, H Sato†, J Harada†, K Miyazaki†, H Namatame†, Y Ueda‡ and M Ohashi‡

† Department of Materials Science, Faculty of Science, Hiroshima University, Kagamiyama 1-3, Higashi-Hiroshima 739, Japan

‡ Tokuyama National College of Technology, Kume-Takajo 3538, Tokuyama 745, Japan

Received 14 February 1995

Abstract. Electronic structures of $Zn_{1-x}Mn_xTe$ films ($0 \leqslant x \leqslant 0.7$) grown epitaxially on GaAs(100) substrates have been investigated by means of *in situ* measurements of conduction band inverse photoemission and valence band photoemission spectra. The inverse photoemission spectrum of pure ZnTe exhibits clear peak structures at 4.0 and 6.7 eV above the valence band maximum, reflecting maxima of density of states of conduction bands. With increasing Mn composition, new peaks show up at 3.5 eV in the inverse photoemission spectra and at -3.7 eV in the photoemission spectra. These peaks are ascribed to emission from the Mn 3d↑ and 3d↓ states with e_g symmetry, respectively, and provide a spin exchange splitting energy of 7.2 ± 0.2 eV. The Mn 3d-derived features are very similar to those in $Cd_{1-x}Mn_xTe$, as a result of the close similarity of the local environment around the Mn atom.

1. Introduction

$Zn_{1-x}Mn_xTe$ mixed crystals belong to the family of diluted magnetic semiconductors (DMSs), in which Mn atoms replace Zn atoms in the zincblende structure for Mn composition (x) up to 0.86 [1, 2]. This system displays many properties analogous with those of the typical DMS of $Cd_{1-x}Mn_xTe$ with identical crystal structure, and has attracted much attention as a new class of semiconductors with novel magnetic [3–8] and optical properties [9–17]. Such phenomena stem from the sp band–Mn 3d and Mn–Mn exchange interactions through the hybridization between the sp band and the Mn 3d states.

Reflectivity spectra of $Zn_{1-x}Mn_xTe$ have been measured as a function of x in the fundamental optical absorption region. Non-linear dependence of the band gap of $Zn_{1-x}Mn_xTe$ on x was interpreted within the framework of sp band–Mn 3d exchange interaction [15]. An x-ray absorption near-edge structure (XANES) study on $Zn_{0.5}Mn_{0.5}Te$ has been performed for the L edge of Te and K edges of Zn and Mn [18]. From the experimental data, values for the Te L_I and L_{III} x-ray absorption edges for a hypothetical zincblende MnTe were extracted and compared with the theoretical result. The maximum contributions of the hybridized unoccupied Mn 3d states have been estimated at about 3.8 and 3.0 eV above the valence band maximum (VBM) for p-projected and s, d-projected densities of states (DOS), respectively. Energy positions of unoccupied Mn 3d↓ states in $Zn_{1-x}Mn_xY$ (Y = Te, Se, S) were inferred from the energy level scheme including energies of Zn 3d core levels, fundamental band gap, main peak of the valence bands, Mn 3p–3d resonance, and Mn 3p core levels [19]. The chemical trend of the Mn 3d spin exchange splitting energy (U_{eff}; the energy necessary to add one electron to a Mn^{2+} ion) has been

0953-8984/95/234371+13$19.50

discussed for $Zn_{1-x}Mn_xY$ (Y = Te, Se, S). However, no direct identification of the Mn 3d↓ states has been reported for $Zn_{1-x}Mn_xTe$ so far.

The contribution of the Mn 3d states to the valence band DOS of $Zn_{0.7}Mn_{0.3}Te$ has been evaluated by means of resonant enhancement of the Mn 3d photionization cross-section near the Mn 3p–3d core excitation using tunable synchrotron radiation [20]. The Mn 3d-derived partial DOS of $Zn_{0.7}Mn_{0.3}Te$ was found to be very similar to that of $Cd_{0.8}Mn_{0.2}Te$. Assuming the local environment around Mn atoms in $Zn_{1-x}Mn_xTe$, the close similarity between the Mn 3d DOSs of $Zn_{1-x}Mn_xTe$ and $Cd_{1-x}Mn_xTe$ was discussed mainly on the basis of the configuration interaction (CI) calculation using an $Mn^{2+}(Te^{2-})_4$ model cluster [21, 22]. The CI analysis confirms a significant Mn 3d–Te 5p hybridization, which allows for sufficient screening of the 3d excitations by the ligand to d hole charge transfer over the top 5 eV region of valence bands. In that sense, the spectral density in the corresponding energy region of valence bands can be assumed to be a good approximation for a measure of the valence band DOS.

The band structure and magnetic properties of Mn-substituted DMSs have been theoretically investigated [23–27] based on a combination of *ab initio* spin-polarized band calculations, a semiempirical tight-binding model containing available experimental data and consideration of alloying effects [23, 24], self-consistent spin-polarized spin density functional band structure calculations [25], spin-polarized, self-consistent local spin density total-energy and band structure calculations [26], and a self-consistent local density pseudofunction theory [27].

In this paper, we present conduction band and valence band spectra of $Zn_{1-x}Mn_xTe$ films ($0 \leqslant x \leqslant 0.7$) grown epitaxially on GaAs(100) substrates, measured by means of ultraviolet inverse photoemission and photoemission spectroscopies (IPES and UPS). The IPES spectra have been successfully obtained, for the first time, by preparing thin epitaxial films on GaAs(100) substrates with very low resistivity to overcome the difficulty of the electrostatic charging effect. *In situ* measurements of IPES and UPS spectra realize a connection of these spectra at the Fermi level [28] and make it possible to determine directly the U_{eff} value to be 7.2 ± 0.2 eV. We discuss the Mn 3d states in $Zn_{1-x}Mn_xTe$ in comparison with the results of band structure calculation in terms of the tight-binding semiempirical coherent potential approximation for $Cd_{1-x}Mn_xTe$ [23], and also with those of the CI calculation using an $Mn^{2+}(Te^{2-})_4$ model cluster [29] in distinction from the one-electron band picture.

2. Experimental details

Figure 1 shows schematically the apparatus used in the present experiments. The IPES spectrometer [30, 31] consists of a low-energy electron gun of Erdman–Zipf type with an energy spread of 0.25 eV, an Al reflection mirror coated with an MgF_2 film, and the bandpass photon detector with a full width at half maximum of 0.47 eV and a maximum response at 9.43 eV. All components are mounted in an ultrahigh-vacuum chamber under a base pressure below 7×10^{-11} Torr. The overall energy resolution of the spectrometer was 0.56 eV. The electron beam was injected normal to the sample surfaces.

The UPS spectrometer connected to the IPES apparatus is composed of an He discharge lamp ($\hbar\omega = 21.2$ eV) and a double-stage cylindrical mirror analyser to obtain angle-integrated spectra. The energy resolution was set to be 0.2 eV. The working pressure of the UPS chamber was 3×10^{-9} Torr under the operation of the discharge lamp, though the base pressure was 4×10^{-10} Torr. Energy calibration of the IPES and UPS spectra were experimentally made using the spectra for a fresh film of polycrystalline Au [31]. The IPES

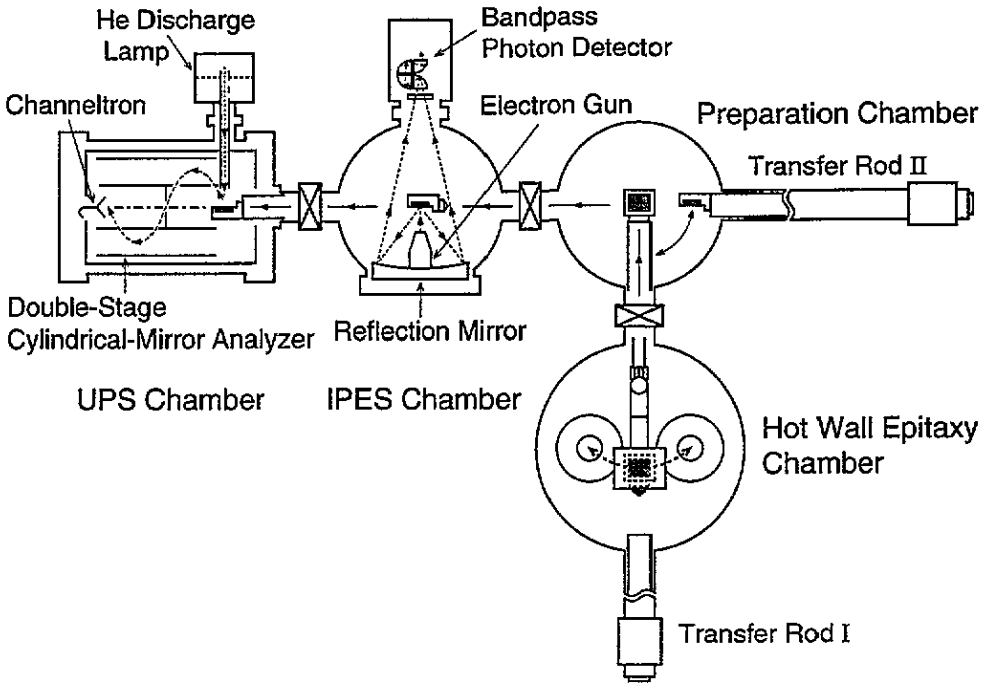

Figure 1. The apparatus used for the IPES and UPS measurements. The IPES spectrometer consists of a low-energy electron gun, an Al reflection mirror coated with an MgF_2 film, the bandpass photon detector with an SrF_2 window and a photomultiplier with the Cu–BeO first dynode coated with a KCl film. The overall energy resolution is 0.56 eV with a maximum response at 9.37 eV. The UPS spectrometer is composed of an He discharge lamp and a double-stage cylindrical mirror analyser.

and UPS spectra measured *in situ* for the same sample surface were connected at the Fermi level.

All measurements of IPES and UPS spectra were carried out at room temperature. The energy was referred to the VBM determined by extrapolating the steep leading edge of the highest valence band peak to the baseline.

Samples used for IPES and UPS experiments were $Zn_{1-x}Mn_xTe$ films (x = 0, 0.2, 0.3, 0.4, 0.6 and 0.7) grown by the hot-wall epitaxy (HWE) technique on (100)-oriented Si-doped n-type GaAs substrates [32] with a misorientation of 2° toward the next [110] direction, and with an impurity concentration of $(1.0–2.5) \times 10^{18}$ cm^{-3} or a resistivity of $(1.5–2.8) \times 10^{-3}$ Ω cm. The HWE reactor consists of a ZnTe furnace with an additional Te source for compensation of the vacancies (hot wall 1) and Mn furnace (hot wall 2), as shown in figure 2(a). A flip-flop method [33] was employed to obtain various thickness and x of films. The thickness was controlled by the repetition number of the flip-flop motion, and x by periods during the stay of substrates over the ZnTe and Mn furnaces operated at 540 and 840 °C, respectively.

Prior to the crystal growth, the substrates were chemically etched in a 5:1:1 solution of H_2SO_4:H_2O_2:H_2O. The substrate, loaded into a vacuum chamber, was heated at 600 °C for 10 min to remove the oxide layer. During the growth, the substrate temperature was kept constant at 350–390 °C depending on x, and the vacuum was $(1–5) \times 10^{-8}$ Torr under the operation of the ZnTe and Mn furnaces. After the growth, the sample was transferred

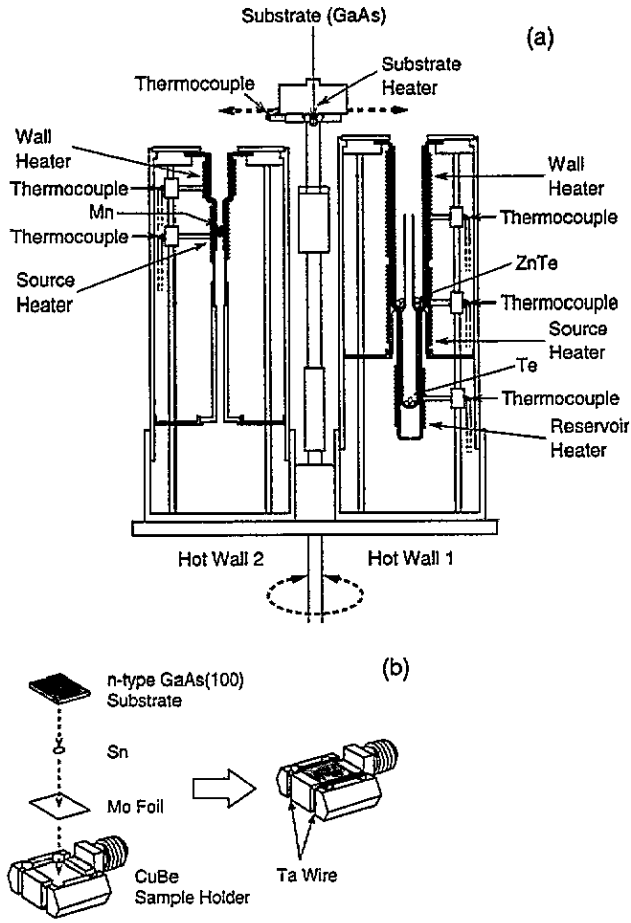

Figure 2. (a) A schematic illustration of the hot-wall reactor, consisting of a ZnTe furnace with an additional Te sources for compensation of the vacancies and an Mn furnace. The thickness of films is controlled by a repetition number of flip-flop motion of the substrate, and x by periods during the stay of the substrate over the ZnTe and Mn furnaces. (b) Details of the sample holder used for the IPES and UPS measurements.

immediately into the preparation chamber under a base pressure below 4×10^{-10} Torr, keeping the substrate temperature above 250 °C, and then introduced into the UPS chamber. In this way, clean surfaces of $Zn_{1-x}Mn_xTe$ epitaxial films were successfully obtained. The crystal structure and x values of epitaxial films with thickness of 0.5–1 μm were checked by x-ray diffraction [34].

The IPES spectra are much more sensitive to an electrostatic charging effect than the UPS spectra [35]. To avoid such an effect, the thickness of the film was reduced by decreasing only the repetition number of the flip-flop motion without changing any other parameters in the growth conditions for the thick $Zn_{1-x}Mn_xTe(100)$ film, until the IPES spectrum exhibited no electrostatic charging effect. The thickness of samples used for the IPES and UPS experiments was measured using a surface profiler (high-precision optical stylus surface measuring instrument, Kosaka Ltd). The typical value of the thickness was about 10–20 nm.

In the present experiments, it is reasonably assumed that the thin films used for the IPES and UPS measurements are (100)-oriented films, since $Zn_{1-x}Mn_xTe$ epitaxial films

with the (100)-orientation grew steadily under suitable parameters mentioned above. The UPS spectra for thin $Zn_{1-x}Mn_xTe$ films, which exhibited no electrostatic charging effect in the IPES measurements, were fully consistent with those for the thick $Zn_{1-x}Mn_xTe(100)$ films. The UPS spectra for thick $Zn_{1-x}Mn_xTe(100)$ films with large enough thickness for determination of orientation using x-ray diffraction were free from the electrostatic charging effect and consistent with those for bulk alloys.

Residual strain is known to be important and affect the electronic structure of ZnTe. The amount of the strain-induced change in energy is, however, estimated to be several tens of millielectronvolts [36, 37] and can be neglected in comparison with the energy resolution of 0.56 and 0.2 eV in the IPES and UPS measurements, respectively.

The x values of the thin epitaxial films were evaluated by x-ray photoemission spectroscopy (XPS; ESCA 5400, Perkin Elmer) using integrated emission intensities of the Zn 2p, Mn 2p, and Te 3d core levels of the epitaxial films, after the IPES and UPS measurements. The XPS spectra for the bulk $Zn_{1-x}Mn_xTe$ specimens with x values determined already by an electron probe microanalysis were used as a reference. The x values evaluated by the XPS measurements for thin epitaxial films were in good agreement with those for thick films estimated from the x-ray diffraction within $x = \pm 0.05$.

Figure 2(b) shows details of the sample holder for the IPES and UPS measurements. Special care was paid to reliable ohmic contacts, which were alloyed onto the back surface of substrate using Sn to avoid an uncontrolled voltage drop at the GaAs wafer–Mo sheet interface. The Mo sheet was used to prevent reaction between the GaAs substrate and CuBe sample holder during the heating process at 600 °C for 10 min.

3. Results and discussion

Figure 3(a) shows the conduction band IPES and valence band UPS spectra of pure ZnTe epitaxial film grown epitaxially on GaAs(100) substrate. These spectra exhibit peak structures at 4.0 and 6.7 eV, and at −1.0, −1.7, −3.2, and −5.1 eV relative to the VBM (vertical bars). In figure 3(b), band structures of ZnTe calculated by Cohen and Bergstresser using the empirical pseudopotential method (thick solid curves) [38], and by Kurganskii and co-workers on the basis of the modified orthogonalized plane wave method (thin solid curves) [39] are presented for the sake of comparison. Energies are referred to the VBM. The direct fundamental band gap is located at the Γ point. The calculated band gap energies of 2.4 [38] and 2.6 eV [39] are slightly larger than the experimental value of 2.3 eV [12, 13].

For the conduction bands, one can recognize flat regions of conduction bands around the L_1, X_1, L_3, and Λ symmetry points, which are located at 3.7, 4.0, 6.8, and 6.5–7.1 eV in the thick solid curves, and 3.5, 3.8, 7.3, and 6.5 eV in the thin solid curves, respectively. These flat regions would make a significant contribution to the DOS peaks of the conduction bands. Thus, we attribute the first peak at 4.0 eV and the second one at 6.7 eV in the IPES spectrum to the DOS features due to flat regions of conduction bands around the L_1 and X_1, and L_3 and Λ symmetry points, respectively.

The valence bands of ZnTe have been previously discussed by several authors in detail. The valence band DOS is primarily composed of the Te 5p states. We recall here that the features at −1.0, −1.7, −3.2, and −5.1 eV (vertical bars) reflect maxima in the DOS of valence bands mainly derived from flat regions around the L_3, X_5, W_2–Σ_1^{min} and W_1 symmetry points, respectively [40, 41]. One notices that features in a pair of IPES and UPS spectra of ZnTe compare well with the results of band structure calculations.

Figure 4 exhibits a series of conduction band IPES and valence band UPS spectra of $Zn_{1-x}Mn_xTe$ films with x of 0, 0.2, 0.3, 0.4, 0.6, and 0.7 [42]. The valence band

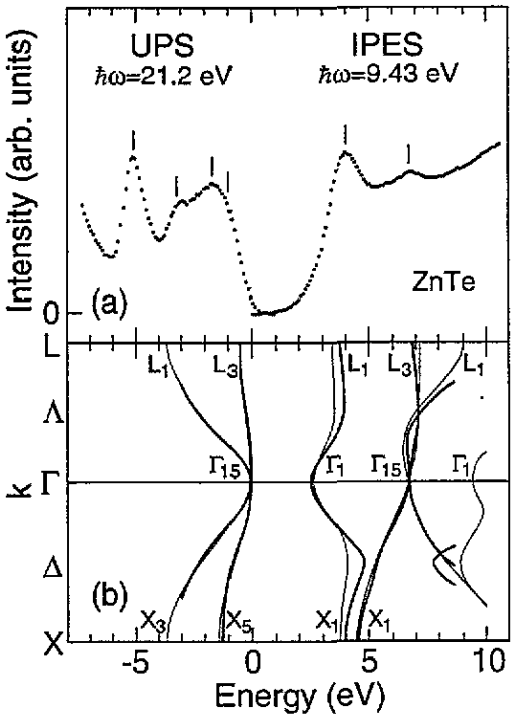

Figure 3. (a) Conduction band IPES and valence band UPS spectra of pure ZnTe epitaxial film grown epitaxially on GaAs(100) substrate. Energies are referred to the VBM. Vertical bars indicate the positions of structures. (b) Energy band structures of ZnTe calculated by Cohen and Bergstresser using the empirical pseudopotential method (thick solid curves) [38], and by Kurganskii and co-workers using the modified orthogonalized plane wave method (thin solid curves [39]).

photoemission spectrum of $Zn_{0.44}Mn_{0.56}Te$ measured at the excitation photon energy of 49.5 eV (on resonance for the Mn 3p–3d core excitation) is also shown to demonstrate the Mn 3d emission with a main peak at −3.7 eV [43]. On increasing x from 0 to 0.3, the width of the first main peak in the IPES spectra increases as a result of an increasing contribution on the lower-energy side of the main peak. For x above 0.4, one notices that a new emission peak shows up clearly at 3.5 eV (vertical solid line), that is, 0.5 eV below the first main peak of ZnTe at 4.0 eV (vertical broken line).

The energy position of the conduction band minimum (CBM) can be roughly evaluated by extrapolating the leading edge of the lowest conduction band peak to the baseline. We find the threshold energy of the IPES spectrum of ZnTe to be 2.3 eV, in good agreement with the band gap energy from experiments on the interband optical transition. The fundamental band gap energy of $Zn_{1-x}Mn_xTe$ is known to increase with x [12, 13], as a result of an increasing contribution of the higher-lying Mn 4s level relative to the Zn 4s level. At $x = 0.7$, the amount of the increase is expected to be about 0.35 eV. Such an increase in the band gap energy is expected to be observed in the form of a higher-energy shift of the threshold with x. One cannot recognize, however, any discernible shift in the experimental spectra. This is probably due to an increasing contribution of the new emission peak at 0.5 eV below the first main peak of ZnTe at 4.0 eV, and also to the characteristics of the overall energy resolution of the IPES spectrometer [44].

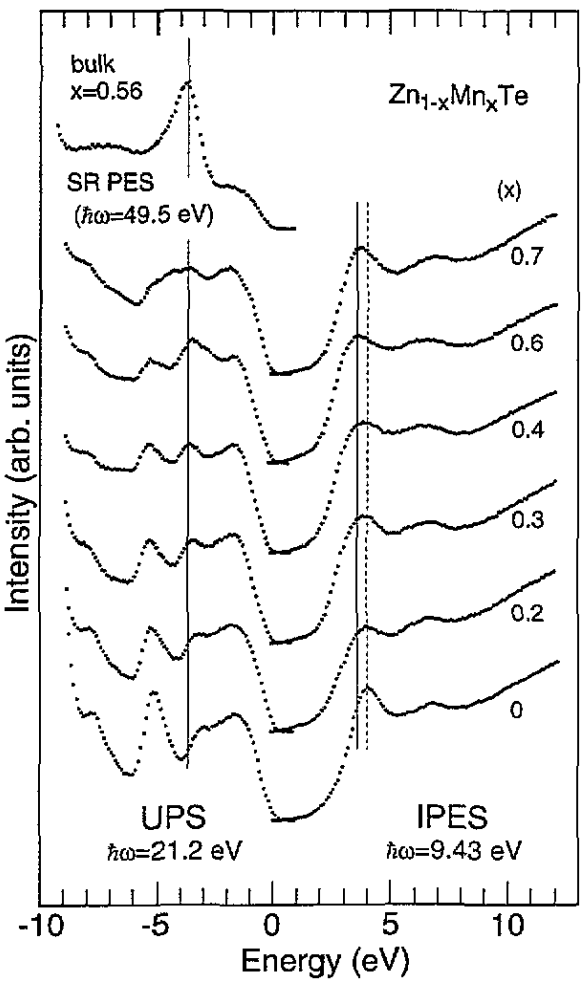

Figure 4. A series of the conduction band IPES and valence band UPS spectra of $Zn_{1-x}Mn_xTe$ films with x values of 0, 0.2, 0.3, 0.4, 0.6, and 0.7. Intensities of the IPES and UPS spectra are tentatively normalized at 12 and −1.7 eV, respectively. The valence band photoemission spectrum of $Zn_{0.44}Mn_{0.56}Te$ measured at the excitation photon energy of 49.5 eV (on resonance) is also shown to demonstrate the Mn 3d emission [43]. Vertical solid lines indicate the positions of Mn-derived new emission peaks, while the vertical broken line represents the position of the main peak in the IPES spectrum of ZnTe.

As concerns the valence band UPS spectra for $Zn_{1-x}Mn_xTe$ with x from 0 to 0.3 [45], we find no remarkable change with respect to energy positions of structures, except for an increasing contribution between −1.7 and −5.1 eV with increasing x. For x above 0.4, however, a new emission peak can be recognized clearly at −3.7 eV. From comparison of these spectra with the valence band spectrum of $Zn_{0.44}Mn_{0.56}Te$ measured at 49.5 eV (on resonance) in figure 4, an increasing spectral density between −1.7 and −5.1 eV with increasing x is found to correspond to the main peak of the spectrum measured at 49.5 eV.

While the Mn 3d features in the UPS spectra are observed as an appreciable increase in intensity at −3.7 eV with x, those in the IPES spectra can be recognized only in the form of an increasing contribution of the new peak 0.5 eV below the main peak of ZnTe. The

Mn 3d features are less pronounced in the IPES spectra than in the UPS spectra. We assume that this is due to the photoabsorption cross-section of the Mn 3d states [46] at 9.43 eV (IPES), smaller by a factor of about three than that at 21.2 eV (UPS).

Very recently, extended x-ray absorption fine-structure (EXAFS) experiments on $Zn_{1-x}Mn_xTe$ performed by Happo *et al* have revealed that the Zn–Te and Mn–Te bond lengths remain almost unchanged for $0 \leqslant x \leqslant 0.65$ [43,47]. The Zn–Te bond length is approximately constant with its value for pure ZnTe, and the Mn–Te bond length is approximately equal to that predicted for the hypothetical zincblende MnTe. In addition, the bond angles of $ZnTe_4$ and $MnTe_4$ clusters are almost independent of x and nearly equal to the 109.8° of a pure tetrahedron, as a result of the strong covalency of the bond between the cation and four coordinated Te. On the Cd–Te and Mn–Te bond lengths, similar results have been previously reported for $Cd_{1-x}Mn_xTe$ by Balzarotti *et al* [48]. That is, the local environment around the Mn atom is very similar between $Zn_{1-x}Mn_xTe$ and $Cd_{1-x}Mn_xTe$. Therefore, we discuss the IPES and UPS spectra of $Zn_{1-x}Mn_xTe$ in comparison with those of $Cd_{1-x}Mn_xTe$, assuming a close similarity between Mn 3d states in $Zn_{1-x}Mn_xTe$ and $Cd_{1-x}Mn_xTe$ alloys.

Figure 5(a) shows the conduction band IPES and valence band UPS spectra of $Zn_{0.3}Mn_{0.7}Te$ and ZnTe films, and the valence band spectrum of $Zn_{0.44}Mn_{0.56}Te$ measured at 49.5 eV (on resonance) [43]. One notices again a main peak at 3.5 eV and a broad and weak structure around 6.5 eV in the IPES spectrum, and valence band structure between 0 and −5 eV with a peak at −3.7 eV in the UPS spectrum, and also a broad satellite between −5 and −9 eV in the spectrum measured at 49.5 eV [43]. For convenience of discussion, an equivalent set of IPES and UPS spectra for $Cd_{0.3}Mn_{0.7}Te$ and CdTe films [49], and the valence band spectrum of $Cd_{0.40}Mn_{0.60}Te$ measured at 49.5 eV (on resonance) [49] is displayed in figure 5(b). In addition, the theoretical total and Mn 3d partial DOSs of CdTe and $Cd_{0.4}Mn_{0.6}Te$ calculated by Ehrenreich *et al* [23] are presented in figure 5(c). The zero of energy in the theoretical DOSs is referred to the VBM of CdTe.

The occupied Mn 3d↑ states in figure 5(c) split into two peaks as a result of sp–d hybridization. The lower states with t_{2g} symmetry hybridize more strongly than the higher states with e_g symmetry in the tetrahedral environment and shift toward lower energy due to a repulsion from the upper Te 5p valence bands. The corresponding 3d admixture in the upper valence band region is responsible for the Mn 3d DOS in the energy region between 0 and −2 eV. The unoccupied Mn 3d↓ states with the e_g symmetry is placed at 3.6 eV above the VBM, just overlapping with the first DOS peak of pure CdTe. The U_{eff} value is taken to be 7.0 eV [23].

For $Cd_{1-x}Mn_xTe$, the main peak at 3.6 eV in the IPES spectra has been assigned to the Mn 3d↓ states with e_g symmetry based on the experimental features of the main peak as well as the comparison between the experiment and theory [49]. Then, the U_{eff} value was estimated to be 7.0 ± 0.2 eV from energy positions of the main peaks in the IPES and UPS spectra (3.6 and −3.4 eV, respectively), in support of the basic validity of the electronic structure model [23,24] for the estimation of the nearest-neighbour Mn–Mn exchange constant (J^{dd}) of $Cd_{1-x}Mn_xTe$, using input parameters such as an energy of occupied Mn 3d states of 3.4 eV taken from photoemission experiments [21,50], $U_{\text{eff}} = 7.0$ eV, a p–d hybridization parameter of $V_{\text{pd}} = 0.219$ eV estimated from the experimental sp–d exchange constant [51], and the Mn–Te bond length of 2.759 Å determined from EXAFS experiments [48].

On the same line of argument on $Cd_{1-x}Mn_xTe$, we assign the main peak at 3.5 eV in the IPES spectrum of $Zn_{0.3}Mn_{0.7}Te$ to the Mn 3d↓ states with e_g symmetry, and evaluate the U_{eff} value to be 7.2 ± 0.2 eV, in combination with the energy position of −3.7 eV for the

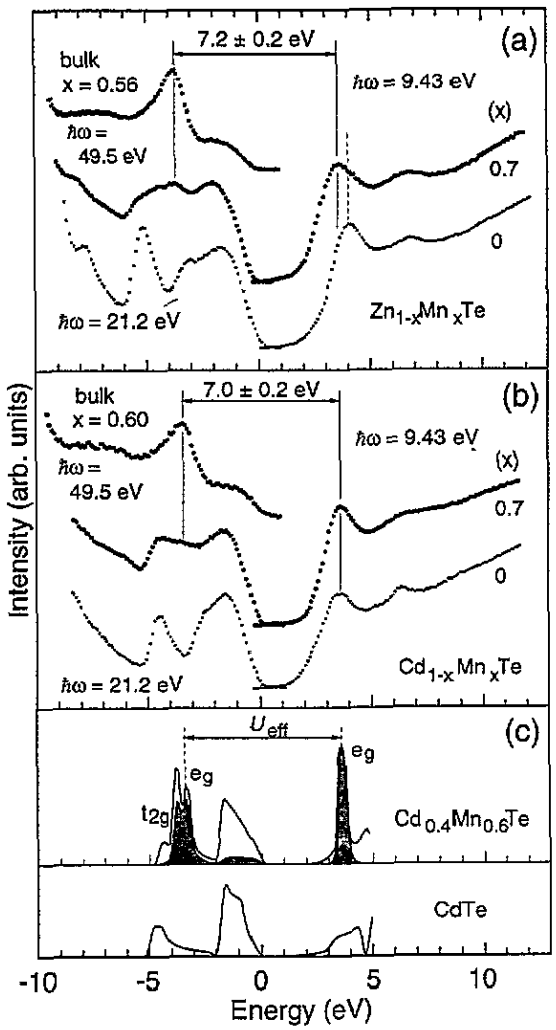

Figure 5. (a) Conduction band IPES and valence band UPS spectra of $Zn_{0.3}Mn_{0.7}Te$ and ZnTe films, and the valence band spectrum of $Zn_{0.44}Mn_{0.56}Te$ measured at 49.5 eV (on resonance) [43]. (b) Conduction band IPES and valence band UPS spectra of $Cd_{0.3}Mn_{0.7}Te$ and CdTe films, and the valence band spectrum of $Cd_{0.40}Mn_{0.60}Te$ measured at 49.5 eV (on resonance) [49]. (c) Total and Mn 3d partial (shaded area) DOSS of $Cd_{0.4}Mn_{0.6}Te$ and the total DOS of CdTe based on the tight-binding calculations [23].

emission due to the Mn 3d↑ states with e_g symmetry in the valence band UPS spectrum. One notices that the U_{eff} value evaluated for $Zn_{1-x}Mn_xTe$ is very close to that for $Cd_{1-x}Mn_xTe$ [49].

Recent first-principles calculations for $Cd_{1-x}Mn_xTe$ by Wei and Zunger predicted the U_{eff} of 4.9 eV [26]. Calculations for paramagnetic zincblende MnTe by Masek *et al* provided a value of 5.5 eV [52] and those for antiferromagnetic zincblende MnTe by Podgórny suggested a value of about 4 eV for the splitting energy [25]. All of the calculated values are substantially smaller than our experimental values of 7.2 ± 0.2 eV for $Zn_{1-x}Mn_xTe$ [53] and 7.0 ± 0.2 eV for $Cd_{1-x}Mn_xTe$ [49]. The U_{eff} value of 5.1 eV for $Zn_{1-x}Mn_xTe$ estimated by Weidemann *et al* [19] seems to be at variance with the present value. There is, however,

no inconsistency, since the value reported for $Zn_{1-x}Mn_xTe$ [19] is only a measure of the lower limit of the exchange energy.

Although there appears a good correspondence between the experiment and energy band theory, the theory can not interpret the multielectron satellite in the energy region between −5 and −9 eV. Nor can it explain the intra-atomic d–d* optical absorption observed at about 2.2 eV for $Zn_{1-x}Mn_xTe$ [9] and $Cd_{1-x}Mn_xTe$ [54].

Recently, the Mn 3d-derived inverse photoemission and photoemission spectra of $Cd_{1-x}Mn_xTe$ have been calculated in terms of the CI theory using an $Mn^{2+}(Te^{2-})_4$ model cluster [29]. Results of the CI calculation for $Cd_{1-x}Mn_xTe$ can be compared to the experimental spectra of $Zn_{1-x}Mn_xTe$ without any change of theoretical parameters, since the local environments around the Mn atom are almost the same [43, 47, 48] as mentioned above.

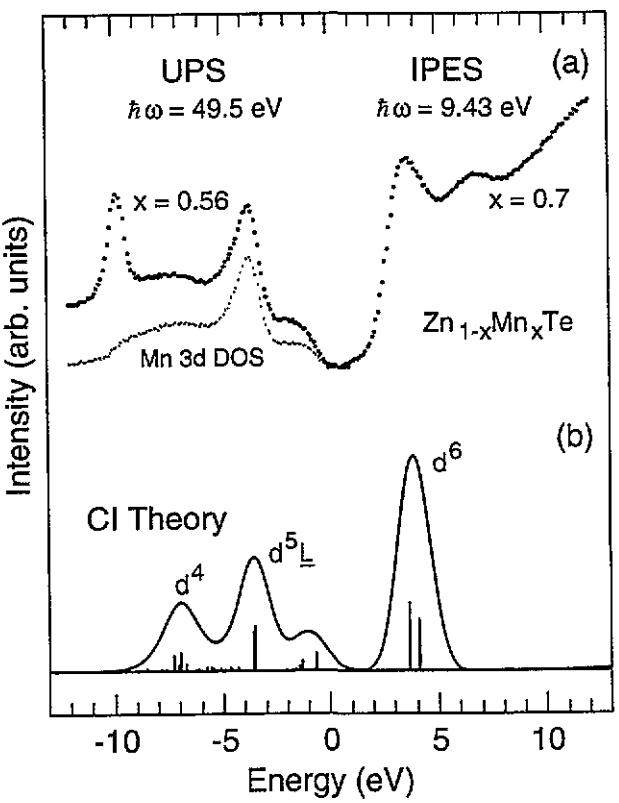

Figure 6. (a) The Conduction band IPES spectrum of $Zn_{0.3}Mn_{0.7}Te$ film, the valence band spectrum of $Zn_{0.44}Mn_{0.56}Te$ measured at 49.5 eV [43], and a measure of the Mn 3d partial DOS of $Zn_{0.44}Mn_{0.56}Te$ evaluated from a resonant photoemission experiment in the Mn 3p–3d core excitation region (dotted curves). (b) Mn 3d-derived inverse photoemission and photoemission spectra of $Cd_{1-x}Mn_xTe$ calculated on the basis of the CI theory [29].

Figure 6 exhibits (a) the conduction band IPES spectrum of $Zn_{0.3}Mn_{0.7}Te$ film, the valence band photoemission spectrum of $Zn_{0.44}Mn_{0.56}Te$ measured at 49.5 eV, and a measure of the Mn 3d partial DOS of $Zn_{0.44}Mn_{0.56}Te$ evaluated from resonant photoemission experiments in the Mn 3p–3d core excitation region [43] (dotted curves), and (b) the Mn 3d-derived

inverse photoemission and photoemission spectra calculated on the basis of the CI theory (solid curves) [29].

For the theoretical Mn 3d photoemission, d^5, $d^6\underline{L}$, $d^7\underline{L}^2$ and d^4, $d^5\underline{L}$, $d^6\underline{L}^2$ configurations are taken into account for the initial and final states, respectively. Here, $\underline{L}$ denotes a ligand hole. The line spectra in figure 6(b) are calculated using parameters of $U = 4.0$ eV, $\Delta = 2.0$ eV, and $(pd\sigma) = -1.1$ eV. Here, U is an averaged Coulomb correlation energy of the Mn 3d electrons ($U \equiv E(3d^4) + E(3d^6) - 2E(3d^5)$, where $E(3d^n)$ is the centre of gravity of the $3d^n$ multiplet) and Δ is the ligand to metal charge transfer energy. In addition, $(pd\sigma)$ represents a p–d transfer integral and $(pd\sigma)/(pd\pi)$ is fixed at -2.16 [55]. The solid curves in figure 6(b) are constructed by a convolution of the line spectra with Gaussian and Lorentzian functions for the sake of comparison.

One can recognize a reasonable agreement between experiment and theory, including the satellite structure between -5 and -9 eV. The comparison reveals that the feature between 0 and -5 eV with a main peak at -3.7 eV is predominantly due to transitions into the $d^5\underline{L}$ final states, whereas the photoemission between -5 and -9 eV is ascribed to transitions into the d^4 final states. In addition, the main peak at 3.5 eV in the Mn 3d inverse photoemission spectrum is attributed to transitions into the d^6 final states.

4. Conclusions

We have measured the conduction band IPES and valence band UPS spectra of $Zn_{1-x}Mn_xTe$ films ($0 \leqslant x \leqslant 0.7$) grown epitaxially on GaAs(100) substrates. The IPES spectrum of pure ZnTe shows peak structures at 4.0 and 6.7 eV with respect to the VBM. On the basis of the results of band structure calculations [38, 39], these structures are ascribed to the DOS features due to particular flat regions of conduction bands around the L_1 and X_1, and L_3 and Λ symmetry points, respectively. The emission observed at 3.5 eV for $Zn_{1-x}Mn_xTe$ films is attributed to the Mn 3d$\downarrow$ states with e_g symmetry. The U_{eff} value is directly estimated to be 7.2 ± 0.2 eV. This value is very close to the 7.0 ± 0.2 eV reported for $Cd_{1-x}Mn_xTe$ [23, 49].

The CI calculations using the $Mn^{2+}(Te^{2-})_4$ model cluster [29] compare well with the Mn 3d-derived features in the IPES and UPS spectra of $Zn_{1-x}Mn_xTe$ films, including the multielectron satellite. The peak at 3.5 eV, features between 0 and -5 eV with a main peak at -3.7 eV, and those between -5 and -9 eV in the Mn 3d partial DOS are assigned to the d^6, $d^5\underline{L}$ and d^4 final states, respectively.

Acknowledgments

The authors are grateful to Professor T Oguchi for stimulating discussions on theoretical aspects, to K Hino and Professor M Hirose for measurements of thickness of epitaxial films, to A Minami for an electron probe microanalysis on bulk specimens, and to N Shimizu for his technical support. This work is partly supported by the Grant-in-Aid for Scientific Research from the Ministry of Education, Science and Culture, Japan, Iketani Science and Technology Foundation, The Ogasawara Foundation for the Promotion of Science and Technology, The Murata Science Foundation, and Shimazu Science Foundation.

References

[1] Furdyna J K and Kossut J (ed) 1988 *Diluted Magnetic Semiconductors, Semiconductors and Semimetals* vol 25 (New York: Academic)

[2] Jain M (ed) 1991 *Diluted Magnetic Semiconductors* (Singapore: World Scientific)

[3] Diouri J, Lascaray J P and Amrani M E 1985 *Phys. Rev.* B **31** 7995

[4] Peterson D L, Bartholomew D U, Debska U, Ramdas A K and Rodriguez S 1985 *Phys. Rev.* B **32** 323

[5] Bruno A and Lascaray J P 1990 *J. Cryst. Growth* **101** 936

[6] Khattak G D, Keith V and Martin P 1992 *Phys. Status Solidi* a **130** 169

[7] Geibultowicz T M, Fernandez-Baca J A, Nicklow R M, Furdyna J K and Debska U 1993 *J. Appl. Phys.* **73** 5660

[8] Soskic Z, Babic Stojic B and Stojic M 1994 *J. Phys.: Condens. Matter* **6** 1261

[9] Morales Toro J E, Becker W M, Wang B I, Debska U and Richardson J W 1984 *Solid State Commun.* **52** 41

[10] Barilero G, Rigaux C, Menant M, Hau N H and Giriat W 1985 *Phys. Rev.* B **32** 5144

[11] Ves S, Strössner K, Gebhardt W and Cardona M 1986 *Phys. Rev.* B **33** 4077

[12] Lee Y R, Ramdas A K and Aggarval R L 1987 *Proc. 18th Int. Conf. on the Physics of Semiconductors* ed O Engstrom (Singapore: World Scientific) p 1759

[13] Debowska D, Kisiel A, Rodzik A, Antonangeli F, Zema N, Piacentini M and Giriat W 1989 *Solid State Commun.* **70** 699

[14] Coquillat D, Lascaray J P, Gaj J A, Deportes J and Furdyna J K 1989 *Phys. Rev.* B **39** 10088

[15] Mertins H-C, Gumlich H-E and Jung C 1993 *Semicond. Sci. Technol.* **8** 1634

[16] Kim Y-G, Kim C-D, Kim H-G, Yang D-I and Kim W-T 1993 *Japan. J. Appl. Phys. Suppl.* **32–33** 590

[17] Hugonnard-Bruyere S, Buss C, Vouilloz F, Frey R and Flytzanis C 1994 *Phys. Rev.* B **50** 2200

[18] Kisiel A, Ali Dahr A-I, Lee P M, Dalba G, Fornasini P and Burattini E 1991 *Phys. Rev.* B **44** 11075

[19] Weidemann R, Gumlich H-E, Kupsch M, Middelmann H-U and Becker U 1992 *Phys. Rev.* B **45** 1172

[20] Tanuguchi M, Soda K, Souma I and Oka Y 1992 *Phys. Rev.* B **46** 15789

[21] Ley L, Taniguchi M, Ghijsen J, Johnson R L and Fujimori A 1987 *Phys. Rev.* B **35** 2839

[22] Taniguchi M, Fujimori A, Fujisawa M, Mori T, Souma I and Oka Y 1987 *Solid State Commun.* **62** 431

[23] Ehrenreich H, Hass K C, Johnson N F, Larson B E and Lampert R J 1987 *Proc. 18th Int. Conf. on the Physics of Semiconductors* ed O Engstrom (Singapore: World Scientific) p 1751

[24] Larson B E, Hass K C, Ehrenreich H and Carlsson A E 1988 *Phys. Rev.* B **37** 4137

[25] Podgórny M 1988 *Z. Phys.* B **69** 501

[26] Wei S-H and Zunger A 1986 *Phys. Rev. Lett.* **56** 2391; 1987 *Phys. Rev.* B **35** 2340

[27] Franciosi A, Wall A, Gao Y, Weaver H J, Tsai M-H, Dow J D, Kasowski R V, Reifenberger R and Pool F 1989 *Phys. Rev.* B **40** 12009

[28] The position of the Fermi level in the band gap of semiconductors depends significantly upon respective samples, while energies of IPES and UPS spectra can be defined experimentally with respect to the Fermi level. Connection of the IPES and UPS spectra at the Fermi level due to *in situ* measurements is essentially important to evaluate accurately the energy separation between the peak in the IPES spectrum and that in the UPS spectrum.

[29] Mizokawa T and Fujimori A 1993 *Phys. Rev.* B **48** 14150
Fujimori A and Mizokawa T 1992 *II–VI Semiconductor Compounds* ed M Jain (Singapore: World Scientific) p 103

[30] Yokoyama K, Nishihara K, Mimura K, Hari Y, Taniguchi M, Ueda Y and Fujisawa M 1993 *Rev. Sci. Instrum.* **64** 87

[31] Ueda Y, Nishihara K, Mimura K, Hari Y, Taniguchi M and Fujisawa M 1993 *Nucl. Instrum. Methods* A **330** 140

[32] Abramof E, Pesek A, Juza P, Sitter H, Fromherz T and Jantsch W 1992 *Appl. Phys. Lett.* **60** 2368

[33] Fujiyasu H, Ishida A, Kuwabara H, Shimomura S, Takaoka S and Murase K 1984 *Surf. Sci.* **142** 579
Suzuki K, Nakamura M, Souma I, Yanata K, Oka Y, Fujiyasu H and Noma H 1992 *J. Cryst. Growth* **117** 881
In the 'flip-flop motion' the GaAs substrate moves from one HWE furnace to the other

[34] Furdyna J K, Giriat W, Mitchell D F and Sproule G I 1983 *J. Solid State Chem.* **46** 349

[35] All bulk samples with x from 0 to 0.65 prepared by a Bridgman method exhibited high resistivity in the range of 10^5–10^8 Ω. Then, the electrostatic charging effect took place inevitably even for an electron beam of 1 μA in our IPES measurements.

[36] Abramof E, Hingerl K, Pesek A and Sitter H 1991 *Semicond. Sci. Technol.* **6** A80

[37] Kudlek G, Presser N, Gutowski J, Hingerl K, Abramof E and Sitter H 1991 *Semicond. Sci. Technol.* **6** A90

[38] Cohen M L and Bergstresser T K 1966 *Phys. Rev.* **141** 789
[39] Kurganskii S I, Farberovich O V and Domashevskaya E P 1980 *Sov. Phys.–Semicond.* **14** 775
[40] Ley L, Pollak R A, McFeely F R, Kowalczyk S P and Shirley D A 1974 *Phys. Rev.* B **9** 600
[41] Shevchik N J, Tejeda J and Cardona M 1974 *Phys. Rev.* B **9** 2627
[42] Intensities of the IPES and UPS spectra are tentatively normalized at 12 and −1.7 eV, respectively. To our knowledge, no evaluation of the absolute intensity of the IPES spectrum or relative intensities among a series of the IPES spectra has been reported so far mainly due to experimental difficulties, though formulation of the method for the background subtraction is in progress (Goodman K W and Henrich V E 1994 *Phys. Rev.* B **49** 4827).
[43] Happo N, Sato H, Mihara T, Mimura K, Hosokawa S, Taniguchi M and Ueda Y 1994 *Proc. 22nd Int. Conf. on the Physics of Semiconductors (Vancouver, 1994)*
The energy position of the main peak of the Mn 3d emission in $Zn_{1-x}Mn_xTe$ is almost independent of x from 0.08 to 0.56
[44] The characteristic curve has an asymmetric feature extending toward lower energy with a full width at half maximum of 0.56 eV [30]. Spectral broadening due to such an instrumental resolution is significant for measurements of the intense and steep edge.
[45] Weak structure at −7.4 eV in the UPS spectrum of ZnTe is due to excitations of the Zn 3d core levels by satellite lines ($\hbar\omega$ = 23.1 and 23.7 eV) of the He I line ($\hbar\omega$ = 21.2 eV). Relative intensities of the satellite lines to the He I line are about 2% or less. With the increase of x, the structure smears out as a result of the decrease of Zn composition in $Zn_{1-x}Mn_xTe$ films.
[46] Yeh J J and Lindau I 1985 *At. Data Nucl. Data Tables* **32** 45, 72
[47] Happo N, Sato H, Hosokawa S, Ueda Y and Taniguchi M 1993 *Japan. J. Appl. Phys. Suppl.* **32–3** 643
[48] Balzarotti A, Cryżyk M, Kisiel A, Motta N, Podgórny M and Zimnal-Starnawska M 1984 *Phys. Rev.* B **30** 2295
Balzarotti A, Motta N, Kisiel A, Zimnal-Starnawska M, Czyżyk M T and Podgórny M 1985 *Phys. Rev.* B **31** 7526
[49] Taniguchi M, Mimura K, Sato H, Harada J, Miyazaki K, Namatame H and Ueda Y *Phys. Rev.* B 51 6932
[50] Taniguchi M, Ley L, Johnson R L, Ghijsen J and Cardona M 1986 *Phys. Rev.* B **33** 1206
[51] Heiman D, Shapira Y and Foner S 1984 *Solid State Commun.* **51** 603
[52] Masek J, Velicky B and Janis V 1986 *Acta Phys. Pol.* A **69** 1107
[53] Our $U_{\rm eff}$ value of 7.2 ± 0.2 eV for $Zn_{1-x}Mn_xTe$ compares well with that of 6.8 eV estimated from the local density functional calculations after correction of the sp band gap to the experimental value [27], though the raw splitting energy before the correction is not available
[54] Lee Y R and Ramdas A K 1984 *Solid State Commun.* **51** 861
[55] Harrison W A 1980 *Electronic Structure and the Properties of Solids* (San Francisco, CA: Freeman) p 451